iScience

CellPress
OPEN ACCESS

Article

Adipocyte-derived chemerin rescues lipid overload-induced cardiac dysfunction

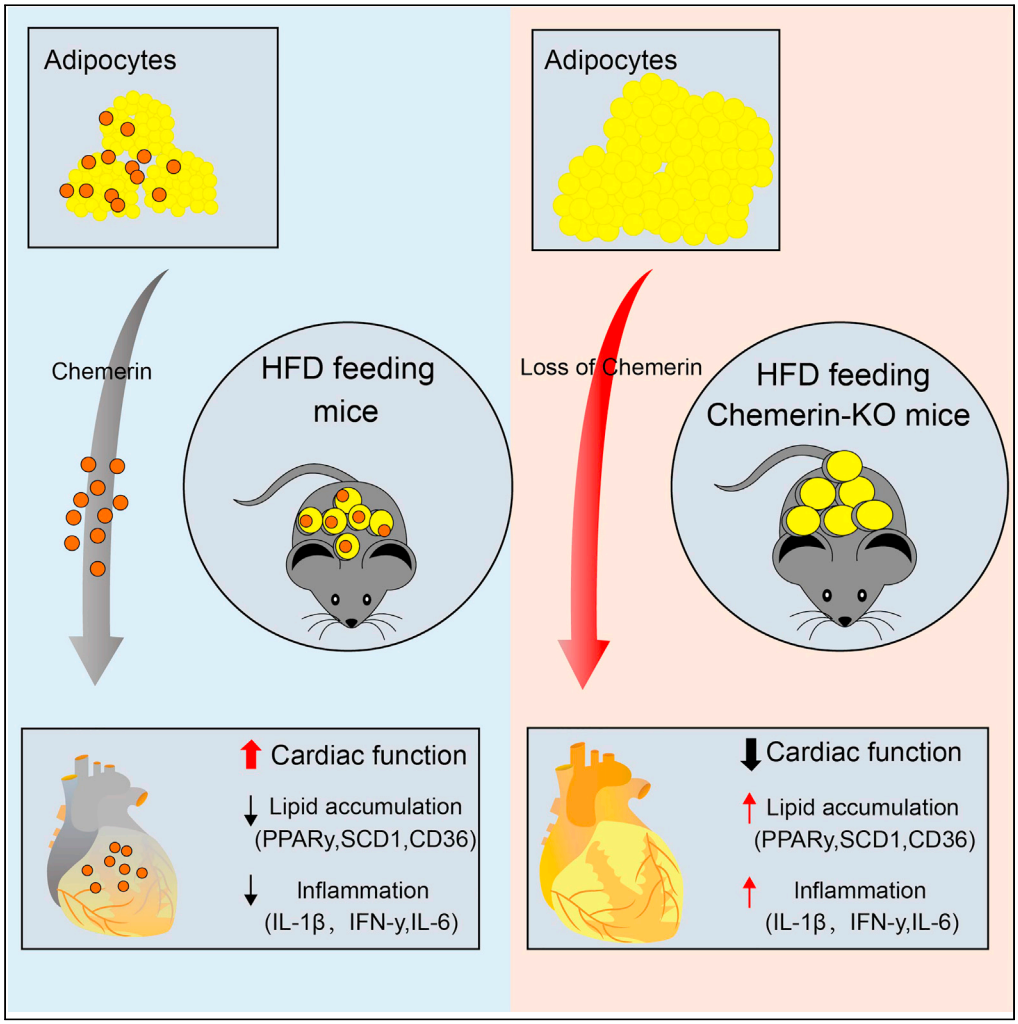

Ruimin Liu, Yinying Han, Chenglong Huang, ..., Shujin Wang, Xi Li, Jie Tian

shujin.wang@cqmu.edu.cn (S.W.)
lixi@shmu.edu.cn (X.L.)
jietian@cqmu.edu.cn (J.T.)

Highlights

Chemerin KO high-fat feeding led to cardiac lipotoxicity, inflammation, and dysfunction

Chemerin lowers lipid accumulation and inflammation in lipid-overloaded cardiomyocytes

Adipocyte-derived endogenous chemerin might protect against obesity-related cardiomyopathy

Liu et al., iScience *26*, 106495
April 21, 2023 © 2023
https://doi.org/10.1016/j.isci.2023.106495

iScience

CellPress
OPEN ACCESS

Article

Adipocyte-derived chemerin rescues lipid overload-induced cardiac dysfunction

Ruimin Liu,[1,2,4] Yinying Han,[2,4] Chenglong Huang,[3] Mengqian Hou,[2] Rui Cheng,[2] Shujin Wang,[2,*] Xi Li,[2,*] and Jie Tian[1,5,*]

SUMMARY

Chemerin, an adipocyte-secreted protein, has been recently suggested to be linked to metabolic syndrome and cardiac function in obese and diabetes mellitus. This study aimed to investigate the potential roles of adipokine chemerin on high fat-induced cardiac dysfunction. Chemerin (*Rarres2*) knockout mice, which were fed with either a normal diet or a high-fat diet for 20 weeks, were employed to observe whether adipokine chemerin affected lipid metabolism, inflammation, and cardiac function. Firstly, we found normal metabolic substrate inflexibility and cardiac function in *Rarres2*$^{-/-}$ mice with a normal diet. Notably, in a high-fat diet, *Rarres2*$^{-/-}$ mice showed lipotoxicity, insulin resistance, and inflammation, thus causing metabolic substrate inflexibility and cardiac dysfunction. Furthermore, by using *in vitro* model of lipid-overload cardiomyocytes, we found chemerin supplementation reversed the lipid-induced abnormalities above. Herein, in the presence of obesity, adipocyte-derived chemerin might function as an endogenous cardioprotective factor against obese-related cardiomyopathy.

INTRODUCTION

Obesity, a worldwide health problem, contributes to lipotoxicity, insulin resistance, and inflammation, all leading to the development of cardiac dysfunction.[1] Obesity-related cardiomyopathy is mainly caused by lipid accumulation in the heart.[2–4] Moreover, this increased lipid accumulation further causes cardiac dysfunction, such as left ventricular hypertrophy, cardiomyocyte stiffness, and reactive interstitial fibrosis.[5] Growing evidence has recently depicted the detrimental effects of dysfunctional adipose tissues on lipotoxicity, insulin resistance, inflammation, and energy substrate utilization in the heart.[6–8] In obesity, adipose tissue-derived factors (or adipocytokines), including adiponectin, leptin, resistin, chemerin, interleukins, tumor necrosis factor alpha (TNF-α), and other inflammatory mediators, change remarkably.[9] Notably, adipocytokines, particularly chemerin, have been suggested to be involved in developing cardiac remodeling in both obese and diabetes via an autocrine, paracrine, or endocrine fashion.[10,11] Accordingly, this raises the possibility that intervention adipokine might be a novel potential treatment approach for obesity-related cardiomyopathy.

Adipokine chemerin is mainly secreted by adipose tissues and the liver. In obesity, adipose tissues produce the most adipokine chemerin in the serum. Chemerin is secreted as a precursor (chem163S) that requires activation extracellularly by proteolytic cleavage.[12,13] In adipocytes, chemerin and its primary receptor, chemokine-like receptor 1 (CMKLR1), are necessary for adipogenesis.[14] Recently, few studies established that the role of the chemerin/chemR23 axis in inflammation is controversial and seems to have both pro-inflammatory and anti-inflammatory properties.[15,16] Of note, an increase in circulating levels of adipokine chemerin in obesity leads to a chronic low-grade inflammatory state that has recently been linked to the development of cardiovascular disease.[17–19] Consistent with this, a negative correlation exists between serum chemerin levels and follow-up time in patients with cardiovascular disease.[18,20,21] Also, chemerin was recently regarded as a biomarker for heart failure.[22,23] With respect to this, little is known about the role of chemerin in the pathogenesis of obesity-related cardiomyopathy. It would be exciting to investigate the potential effects of adipokine chemerin on obesity-related cardiomyopathy.

In this investigation, we found that an increase of serum chemerin in HFD mice, which is mainly released in adipose tissues, induced CMKLR1 to express its primary receptor. This early occurrence may protect against cardiomyopathy brought on by obesity. Chemerin knockout mice were created to confirm this

[1]Department of Cardiology, Children's Hospital of Chongqing Medical University, National Clinical Research Center for Child Health and Disorders, Ministry of Education Key Laboratory of Child Development and Disorders, Chongqing 400032, PR China

[2]Biology Science Institutes, Chongqing Medical University, Chongqing 400032, PR China

[3]Department of Clinical Laboratory, University-Town Hospital of Chongqing Medical University, Chongqing 400032, PR China

[4]These authors contributed equally

[5]Lead contact

*Correspondence: shujin.wang@cqmu.edu.cn (S.W.), lixi@shmu.edu.cn (X.L.), jietian@cqmu.edu.cn (J.T.)

https://doi.org/10.1016/j.isci.2023.106495

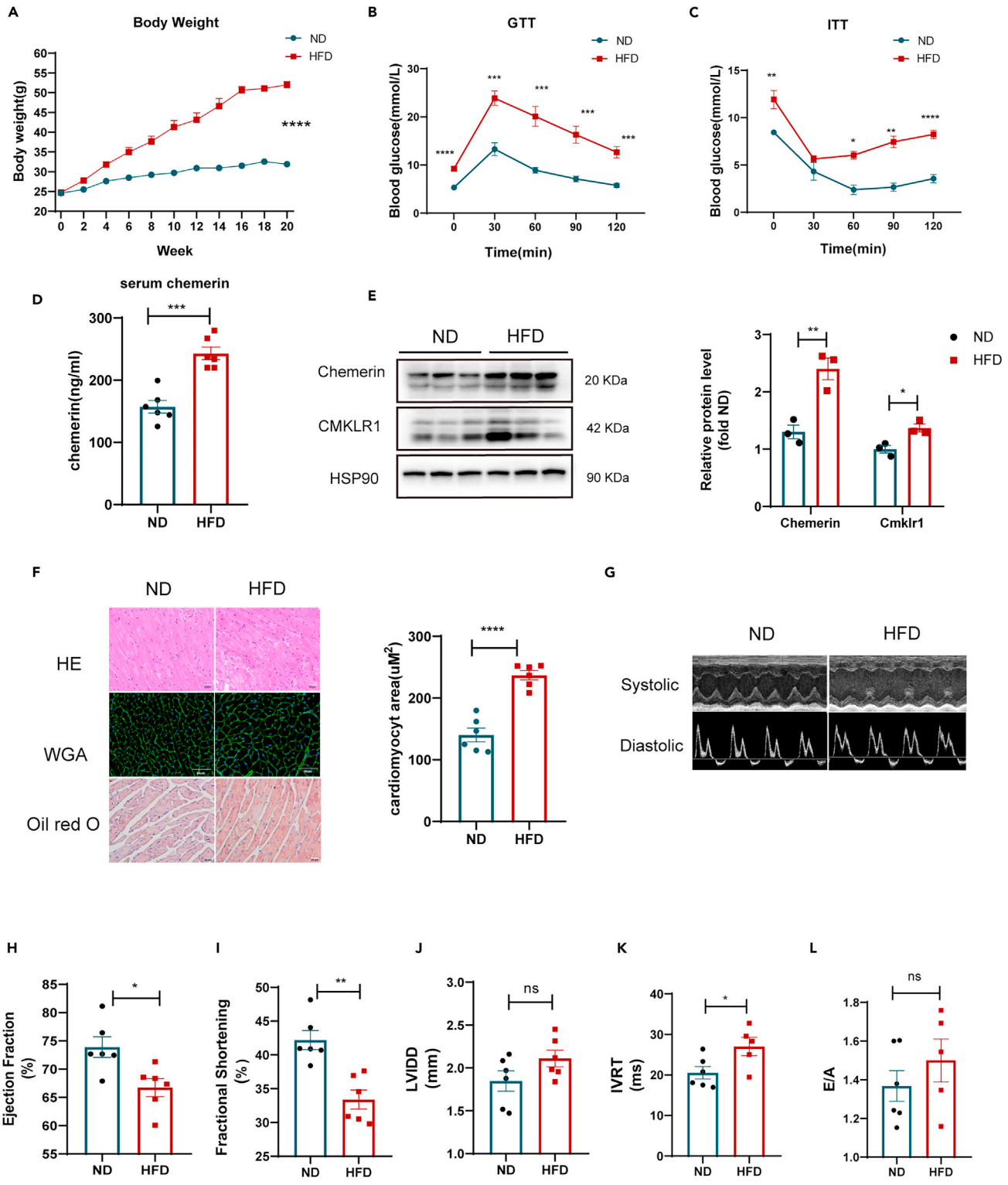

Figure 1. Increased serum chemerin was associated with insulin resistance and cardiac dysfunction in HFD mice

WT mice were subjected to normal diet (ND) or high-fat diet (HFD) feeding for 20 weeks.

(A) Body weight of ND and HFD mice n = 6.

(B and C) Glucose tolerance tests (GTTs) and insulin tolerance tests (ITTs) were performed in ND and HFD WT mice. *p < 0.05, **p < 0.01, HFD vs. ND n = 6.

Figure 1. *Continued*

(D) The levels of serum chemerin in both ND and HFD mice n = 6.

(E) Western blots and its quantification of chemerin and its main receptor (CMKLR1) in the heart. The HSP90 was used as a loading control (n = 3). *p < 0.05, **p < 0.01, HFD vs. ND.

(F) Representative cross-sections of the heart that were stained with Hematoxylin and Eosin (H&E), Wheat Germ Agglutinin (WGA), and Oil red O (ORO), and the quantification of cardiomyocyte sizes with WGA staining. ****p < 0.0001, HFD vs. ND, n = 6, scale bar = 50μm.

(G) Representative systolic and diastolic echocardiography images of ND and HFD mice.

(H–L) E/A ratio, isovolumic relaxation time (IVRT), fractional shortening (FS), Left ventricular ejection fraction (LVEF), diastolic left ventricular internal dimension (LVID; D) were measured by echocardiography. *p < 0.05, **p < 0.01, HFD vs. ND, n = 6.

notion. When they were fed a high-fat diet, it was shown that the Rarres2 knock further generated lipotoxicity, which caused inflammation, glucose/insulin resistance, and cardiac dysfunction. Nevertheless, these abnormalities above were not observed in *Rarres2*$^{-/-}$ mice under normal-diet feeding. Furthermore, using lipid-overloaded cardiomyocytes, we observed that chemerin supplementation lowered lipid accumulation, insulin resistance, and inflammation. Next, knocking down the *CMKLR1* gene could abolish these protective effects of chemerin in lipid-overloaded cardiomyocytes. Herein, our data demonstrate that adipocyte-derived chemerin functions as a critical protective regulator of cardiac function in the obese/or pre-diabetic heart.

RESULTS

Adipocyte-derived chemerin is involved in amending obesity-related cardiomyopathy

We first confirmed that, in comparison to other tissues (such as skeletal muscle, the heart, and the liver) of mice receiving high-fat diets, chemerin was highly expressed in adipose tissue, which includes both subcutaneous fat (SAT) and visceral fat (VAT). This is because chemerin is primarily produced by adipose tissue (Figure S1A). Intriguingly, skeletal muscle and heart muscle both generated large amounts of chemerin's primary receptor (CMKLR1) despite adipose tissue having modest levels of expression (Figures S1A and S1B). It implies that the heart may be one of the organs that adipokine chemerin targets.

Next, we looked into whether elevated serum chemerin in mice receiving high-fat diets affected lipid accumulation, insulin sensitivity, and heart function (Figure 1). As anticipated, HFD mice had considerably higher serum chemerin levels and expression of chemerin/its receptor (CMKLR1) when compared to ND mice (Figures 1D and 1E). A higher body weight (Figure 1A), impaired GTT/ITT (Figures 1B and 1C), excessive lipid buildup (Oil red O staining) (Figure 1F), and heart hypertrophy (HE/WGA staining) were also associated with this elevated chemerin (Figure 1F). Furthermore, by using the echocardiography analysis for mice (Figures 1H-1L), we also observed that high-fat feeding resulted in cardiac dysfunction, such as decreased ejection fraction (EF) and fractional shortening (FS), increased diastolic left ventricular internal dimension (LVID; D). These data obtained together demonstrate that adipokine chemerin is potentially involved in amending obesity-related cardiomyopathy.

Chemerin deficiency does not cause obesity-related cardiomyopathy in healthy mice

To address the hypothesis above, chemerin knockout (*Rarres2*$^{-/-}$) mice were employed in this study. First, there was no significant difference in body weight in *Rarres2*$^{-/-}$ mice and WT littermates under normal-diet feeding for 20 weeks (Figure 2A). It did not lead to an impairment of GTT/ITT (Figures 2B and 2C). The fasting serum levels of NEFA and TG in *Rarres2*$^{-/-}$ mice were similar to WT littermate mice, while TC, HDL-c, and No-HDL-c in *Rarres2*$^{-/-}$ mice are higher than WT littermate. (Figures 2D-2H). Also, there were no differences in lipid accumulation (Oil red O staining), cardiac hypertrophy (HE/WGA staining) (Figure 2I), and cardiac function (e.g., EF, FS, LVIDD, IVRT, and E/A) between WT littermate mice and *Rarres2*$^{-/-}$ mice (Figures 2K–2O).

Chemerin deficiency contributes to obesity-related cardiomyopathy in obese mice

On the contrary, under high-fat diet feeding for 20 weeks, *Rarres2*$^{-/-}$ mice resulted in fast-growing body weight and impairments of GTT/ITT (Figures 3A–3C), excessive lipid accumulation (Oil red O staining) (Figure 3D), cardiac hypertrophy (HE/WGA staining). Furthermore, we discovered that *Rarres2*$^{-/-}$ mice were more susceptible to heart dysfunction than their littermates (such as decreased ejection fraction and fractional shortening, increased diastolic left ventricular internal dimension, and decreased E/A ratio) when fed a high-fat diet (Figures 3F–3J). According to the findings above, obesity-related cardiomyopathy is associated with the loss of adipokine chemerin in obese mice.

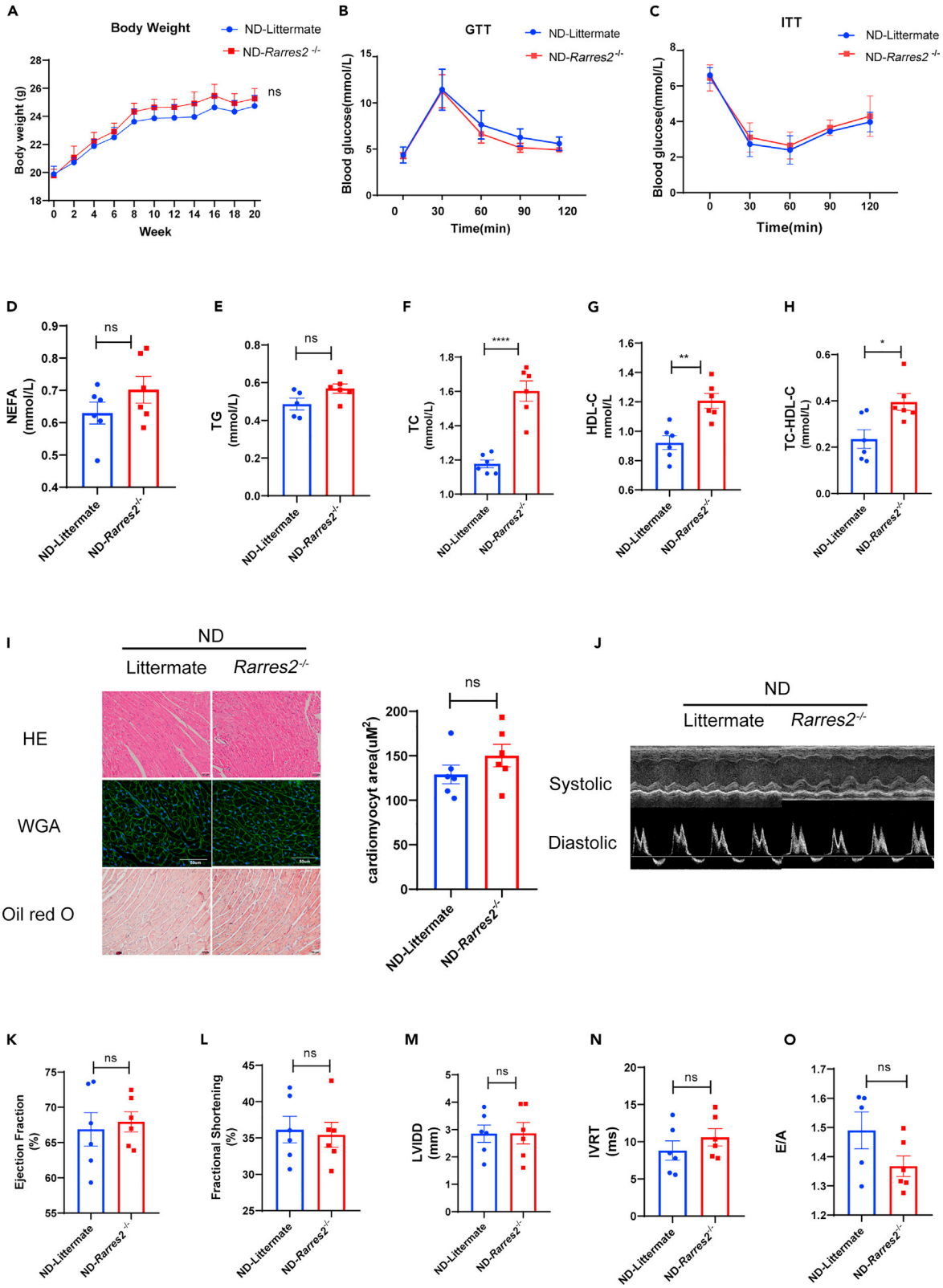
A
Body Weight
ND-Littermate
ND-Rarres2 -/-
Body weight (g)
Week
ns
B
GTT
ND-Littermate
ND-Rarres2-/-
Blood glucose(mmol/L)
Time(min)
C
ITT
ND-Littermate
ND-Rarres2 -/-
Blood glucose(mmol/L)
Time(min)
D
NEFA (mmol/L)
E
TG (mmol/L)
F
TC (mmol/L)
****
G
HDL-C mmol/L
**
H
TC-HDL-C (mmol/L)
*
I
ND
Littermate
Rarres2-/-
HE
WGA
Oil red O
cardiomyocyt area(uM2)
J
ND
Littermate
Rarres2-/-
Systolic
Diastolic
K
Ejection Fraction (%)
L
Fractional Shortening (%)
M
LVIDD (mm)
N
IVRT (ms)
O
E/A
ND-Littermate
ND-Rarres2-/-

Figure 2. Chemerin knockout mice had normal metabolic markers and cardiac function when fed a normal diet

Rarres2$^{-/-}$ and littermate WT mice were fed with normal diet for 20 weeks.

(A) Body weight of *Rarres2*$^{-/-}$ and littermate WT mice, n = 6.

(B and C) Measurement of GTT and ITT in *Rarres2*$^{-/-}$ and littermate WT mice, n = 6.

(D-H) Overnight fasted serum non-esterified fatty acid (NEFA), triglyceride (TG), total cholesterol (TC), HDL-C, and No HDL-C levels, n = 6, *p < 0.05, **p < 0.01, ****p < 0.0001, *Rarres2*$^{-/-}$ vs. littermate (I) Representative cross-sections of the hearts stained with H&E WGA and Oil-Red O staining and its quantification of cardiomyocyte sizes with WGA staining, n = 6, *Rarrres2*$^{-/-}$ vs. Littermate, scale bar = 50μm.

(J) Representative systolic and diastolic echocardiography images in *Rarres2*$^{-/-}$ and littermate mice.

(K-O) Left ventricular function assessed by E/A ratio, isovolumic relaxation time (IVRT), fractional shortening (FS), Left ventricular ejection fraction (LVEF), diastolic left ventricular internal dimension (LVID; D), n = 6.

Chemerin deficiency increases myocardial inflammation in obese mice

Given that obesity-related cardiomyopathy was accompanied by an evoked inflammation in the heart, we further analyzed whether chemerin deficiency increases myocardial inflammation in HFD mice. First, we found that the expression of serum chemerin in *Rarres2*$^{-/-}$ was significantly lowered when compared with Littermate WT mice (Figure 4A). Next, mRNA expressions of pro-inflammatory cytokines (e.g., *TNF-α, IFN-γ. IL-1β,* and *IL-6*) were significantly increased in *Rarres2* knockout mice compared with those of WT mice (Figure 4B). Being consistent with this, the expression of inflammatory-related proteins (e.g., phosphorylation of p65 NF-κB and p38 MAPK) were also remarkably upregulated with chemerin deficiency (Figure 4C).

Chemerin deficiency accelerates cardiac metabolic dysfunction in HFD mice

Using indirect calorimetric measurement, the whole energy expenditure of both littermate and *Rarres2*$^{-/-}$ mice was investigated in this study. Under high-fat diet feeding, there was no significant difference in O_2 production (Figure 5A) and CO_2 production (Figure 5B) during the light/dark phase between WT and *Rarres2*$^{-/-}$ mice. Notably, when compared with WT mice, a lower respiratory exchange ratio (RER) was observed in *Rarres2*$^{-/-}$ mice (Figure 5C). Also, after food ingestion during the dark phase, an increasement in locomotor activity was observed in *Rarres2*$^{-/-}$ mice after food ingestion during the dark phase (Figure 5D). Therefore, concerning this energy substrate utilization, it suggested that a shift to fatty acids in *Rarres2*$^{-/-}$ mice.

Next, the serum levels of triglyceride (TG), total cholesterol (TC), non-esterified fatty acid (NEFA), and high-density lipoprotein cholesterol (HDL-C) in both WT mice and *Rarres2*$^{-/-}$ mice under high-fat diet feeding were also measured in this study. As shown in (Figures 5E–5I), TG, TC, and NEFA were significantly increased in *Rarres2*$^{-/-}$ mice compared with those of WT mice ($p < 0.05$). However, no significant differences were found in HDL-C between WT mice and *Rarres2*$^{-/-}$ mice.

Also, using non-targeted metabolomics, the effect of knocking out *Rarres2* on the metabolism of small molecule intermediates in the heart of HFD mice was investigated. The PCA analysis showed that the metabolites in the heart were significantly separated between WT mice and *Rarres2*$^{-/-}$ mice, with the first two principal component scores of PC1 and PC2 being 57% and 54%, respectively. According to the analysis of the heatmap, it also showed that knocking out *Rarres2* in HFD mice upregulated some lipid metabolites/intermediates, such as stearic acid (18:0), palmitic acid (16:0), adrenic acid (Ada) (Figure 5J). Furthermore, the results of top metabolic pathways enriched classification and annotation illustrated that these lipid metabolites were mainly enriched in fatty acid biosynthesis, α-Linolenic acid biosynthesis, and beta-oxidation of long-chain fatty acids (Figure 5K). Thus, these data suggest that knocking out *Rarres2* in HFD mice results in upregulated expression of genes related to lipid accumulation.

Finally, by using RT-qPCR, we validated whether knocking out *Rarres2* in HFD mice on mRNA expressions of key enzymes, which are involved in lipid uptake, FA synthesis, TG synthesis, and FA oxidation. And, we found that mRNA expressions of most genes (e.g., *ACC, PPARα, PPARγ, FASN, LACD, SREBPs, CPT1, DGAT1-2, LXRα, MCD,* and *CD36*) were significantly upregulated with knocking out *Rarres2* (Figure 5L). Furthermore, key enzymes of lipogenes*is su*ch as PPARγ and SCD1 were detected using Western blot, and it indicated that both PPARγ and SCD1 were significantly increased in *Rarres2*$^{-/-}$ mice (Figure 5M). Taken together, the loss of chemerin in HFD mice results in a significant shift in lipid metabolism, and it suggests that adipokine chemerin amends obesity-related cardiomyopathy.

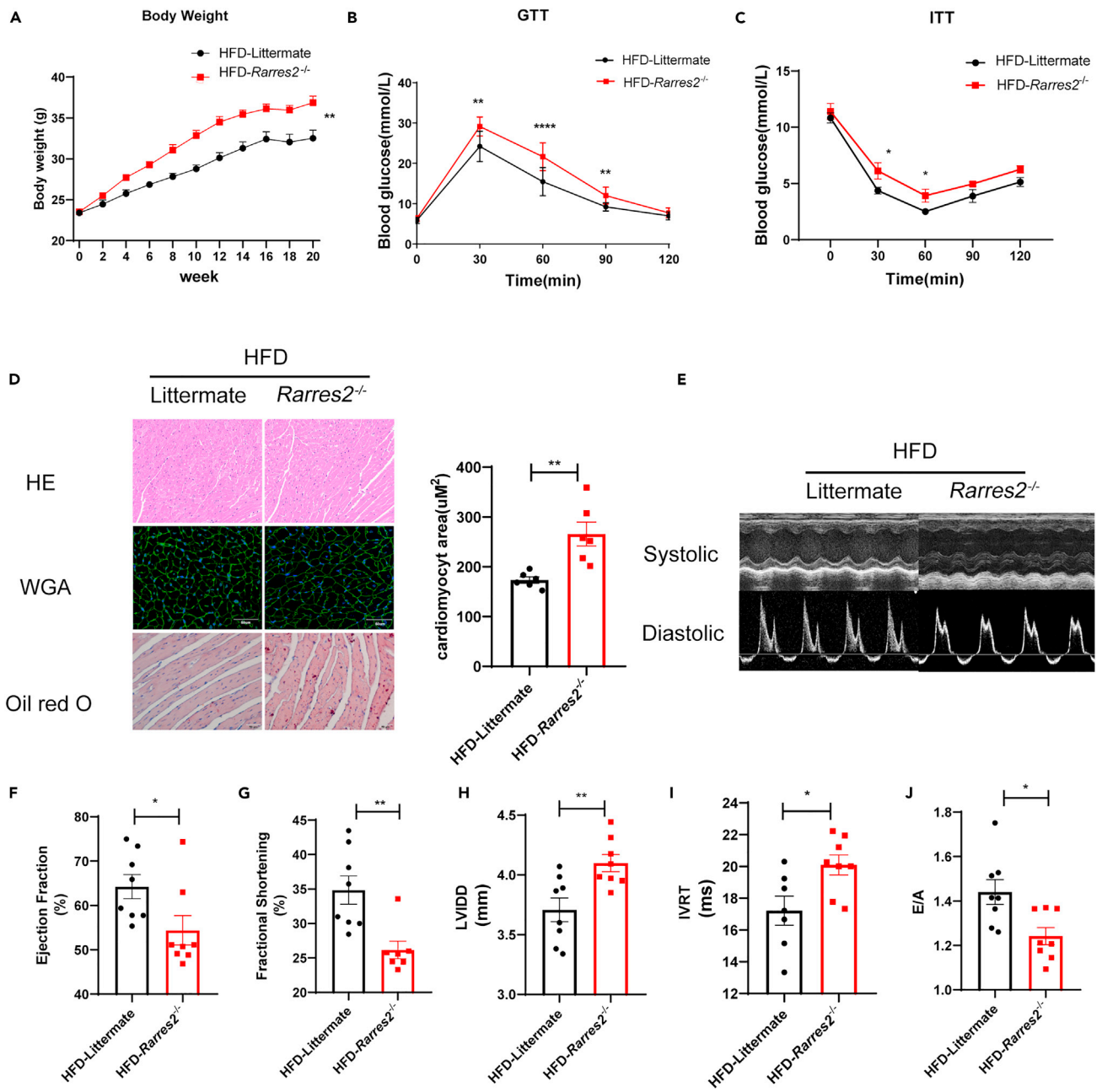

Figure 3. Chemerin knockout exacerbated cardiac remodeling in HFD mice

Rarres2$^{-/-}$ and Littermate WT mice were subjected to high-fat diet feeding for 20 weeks.

(A) Body weight of two groups, n = 8 (B and C) Glucose tolerance test (GTT) and insulin tolerance test (ITT) were performed in *Rarres2*$^{-/-}$ and littermate mice. *p < 0.05, **p < 0.01, *Rarres2*$^{-/-}$ vs. littermate, n = 8.

(D) Representative cross-section of hearts stained for H&E, WGA, and Oil-Red O staining, its quantitative analysis of cardiomyocyte size (WGA staining). *p < 0.05, *Rarrres2*$^{-/-}$ vs. Littermate, n = 6, scale bar = 50μm.

(E) Representative systolic and diastolic echocardiography images of littermate and *Rarres2*$^{-/-}$ mice.

(F-J) Left ventricular function of littermate and *Rarres2*$^{-/-}$ in HFD, assessed by Left ventricular ejection fraction (LVEF), fractional shortening (FS), diastolic left ventricular internal dimension (LVID; D), E/A ratio, and isovolumic relaxation time (IVRT). *p < 0.05, **p < 0.01, *Rarres2*$^{-/-}$ vs. littermate, n = 8.

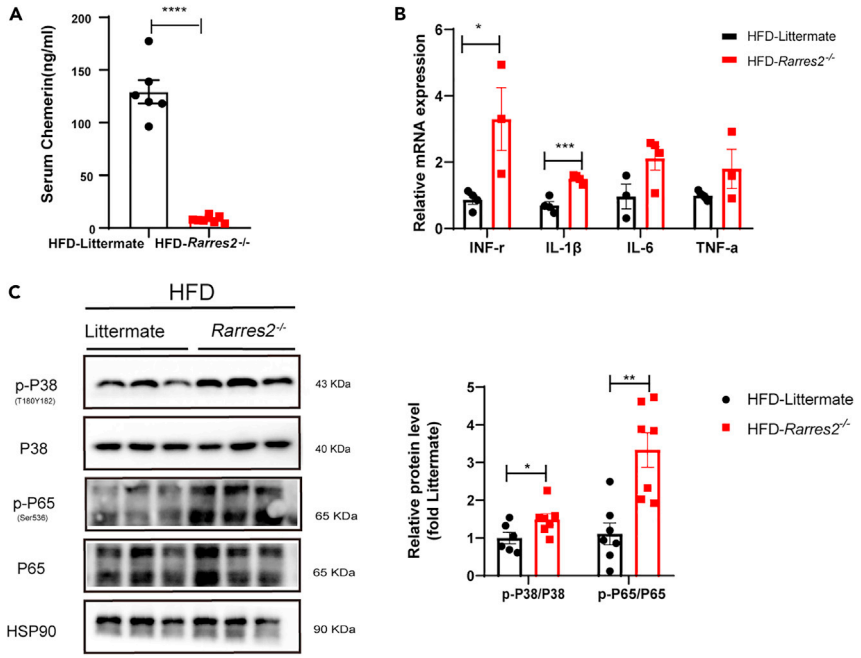

Figure 4. chemerin knockout increased pro-inflammatory cytokines in the heart of HFD mice

Rarres2$^{-/-}$ and *Littermate* WT mice were subjected to high-fat diet feeding for 20 weeks.

(A) Serum chemerin level was detected by ELISA in both *Rarres2*$^{-/-}$ and Littermate mice, n = 6.

(B) The RT-qPCR analysis of pro-inflammatory cytokines in the heart between *Rarres2*$^{-/-}$ and littermate WT mice, n = 3.

(C) Western blots and its quantification of p-P38, P38, and p-P65, P65 in the heart. The HSP90 was used as a loading control (n = 6). *p < 0.05, **p < 0.01, ***p < 0.001.

Chemerin supplementation amends lipid overload-induced lipotoxicity and inflammation in cardiomyocytes

According to the findings above, we further investigate whether chemerin supplementation rescues lipid overload-induced lipotoxicity and inflammation in neonatal mouse primary cardiomyocytes (NMCMs). First, by using Oil red O staining, we found that chemerin supplementation (200 ng/ml for 24h, PeproTech,300-66) significantly lowered lipid accumulation in lipid-overload NMCMs, and this beneficial effect was completely abolished by knocking down its main receptor (*CMKLR1*) (Figure 6A). Being consistent with *in vivo* results (Figure 5M), when compared with high palmitate (HP) condition, the lower protein expression of key lipid synthesis protein (e.g., PPARγ, *SCD1*) was observed in the HP/chemerin condition (Figure 6B). And, knocking down *CMKLR1* also completely blocked these effects.

Considering insulin signaling, phosphorylation levels of Akt (*p*-Akt Ser473) were assessed in this study. In agreement with *in vivo* findings, lipid-overload cardiomyocytes showed a loss of insulin-stimulated phosphorylation of Akt, and chemerin supplementation could restore this lipid-induced loss of insulin-stimulated Akt phosphorylation (Figure 6C). Additionally, we also found that in lipid-overload cardiomyocytes, chemerin supplementation significantly lowered mRNA expressions of (e.g., *TNF-α* and *IFN-γ*) in lipid-overload cardiomyocytes (Figures 6D and 6E). Notably, these beneficial effects of chemerin on insulin sensitivity and pro-inflammatory cytokines in lipid-overload cardiomyocytes were almost inhibited by knocking down *CMKLR1*.

Together with both *in vitro* and *in vivo* findings, adipocyte-derived chemerin can rescue lipid overload-induced lipotoxicity, insulin resistance, inflammation, and cardiac dysfunction.

DISCUSSION

Obesity is known to be the main risk factor for the development of new-onset heart failure, and approximately 50% of individuals with obesity have heart failure with preserved ejection fraction (HFpEF).[24]

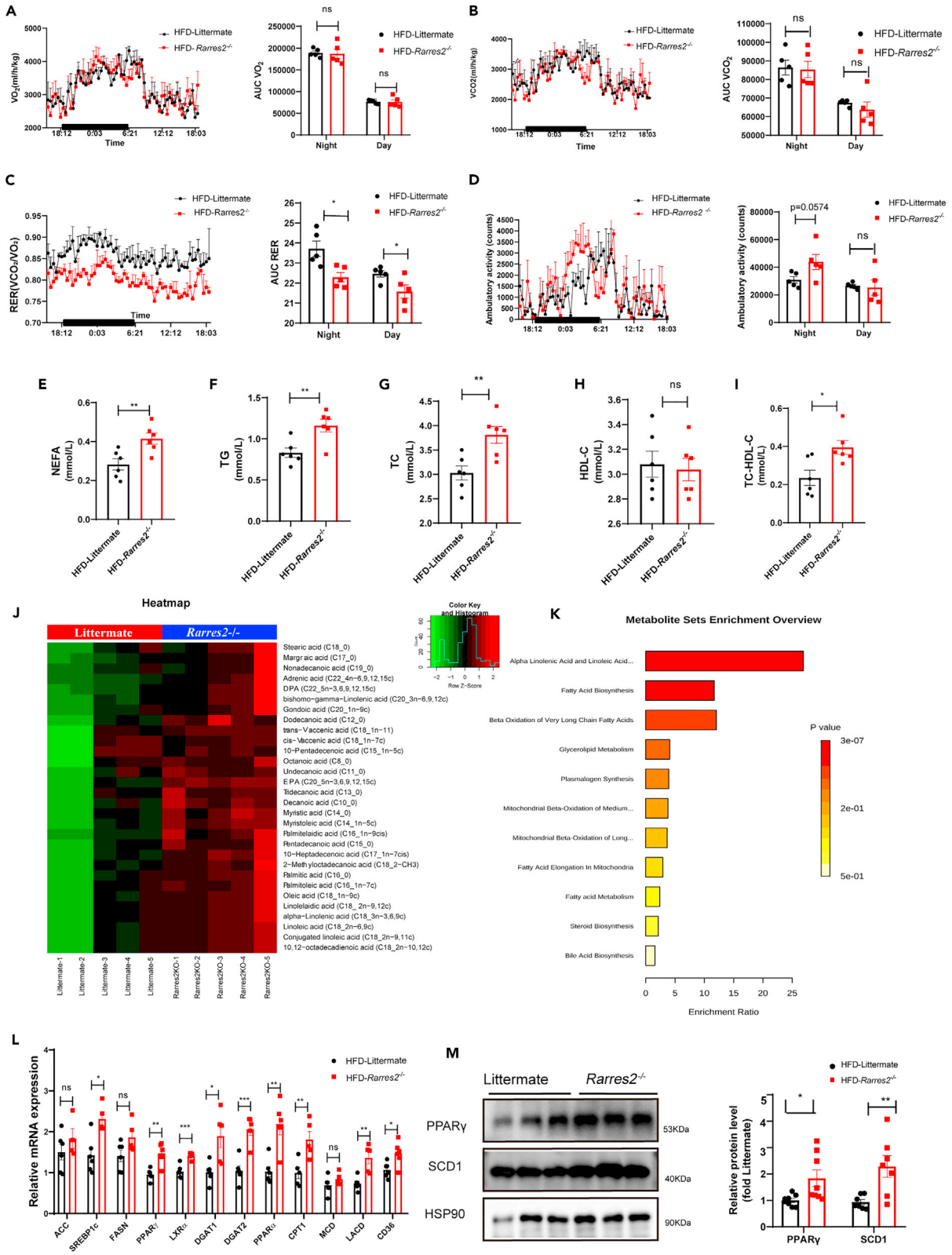
A
HFD-Littermate
HFD-Rarres2-/-
VO2(ml/h/kg)
Time
AUC VO2
Night
Day
ns
B
VCO2(ml/h/kg)
AUC VCO2
C
RER(VCO2/VO2)
AUC RER
D
Ambulatory activity (counts)
p=0.0574
E
NEFA (mmol/L)
F
TG (mmol/L)
G
TC (mmol/L)
H
HDL-C (mmol/L)
I
TC-HDL-C (mmol/L)
J
Heatmap
Littermate
Rarres2-/-
Color Key and Histogram
Row Z-Score
Stearic acid (C18_0)
Margaric acid (C17_0)
Nonadecanoic acid (C19_0)
Adrenic acid (C22_4n-6,9,12,15c)
DPA (C22_5n-3,6,9,12,15c)
bishomo-gamma-Linolenic acid (C20_3n-6,9,12c)
Gondoic acid (C20_1n-9c)
Dodecanoic acid (C12_0)
trans-Vaccenic acid (C18_1n-11)
cis-Vaccenic acid (C18_1n-7c)
10-Pentadecenoic acid (C15_1n-5c)
Octanoic acid (C8_0)
Undecanoic acid (C11_0)
EPA (C20_5n-3,6,9,12,15c)
Tridecanoic acid (C13_0)
Decanoic acid (C10_0)
Myristic acid (C14_0)
Myristoleic acid (C14_1n-5c)
Palmitelaidic acid (C16_1n-9cis)
Pentadecanoic acid (C15_0)
10-Heptadecenoic acid (C17_1n-7cis)
2-Methyloctadecanoic acid (C18_2-CH3)
Palmitic acid (C16_0)
Palmitoleic acid (C16_1n-7c)
Oleic acid (C18_1n-9c)
Linolelaidic acid (C18_2n-9,12c)
alpha-Linolenic acid (C18_3n-3,6,9c)
Linoleic acid (C18_2n-6,9c)
Conjugated linoleic acid (C18_2n-9,11c)
10,12-octadecadienoic acid (C18_2n-10,12c)
Littermate-1
Littermate-2
Littermate-3
Littermate-4
Littermate-5
Rarres2KO-1
Rarres2KO-2
Rarres2KO-3
Rarres2KO-4
Rarres2KO-5
K
Metabolite Sets Enrichment Overview
Alpha Linolenic Acid and Linoleic Acid...
Fatty Acid Biosynthesis
Beta Oxidation of Very Long Chain Fatty Acids
Glycerolipid Metabolism
Plasmalogen Synthesis
Mitochondrial Beta-Oxidation of Medium...
Mitochondrial Beta-Oxidation of Long...
Fatty Acid Elongation In Mitochondria
Fatty acid Metabolism
Steroid Biosynthesis
Bile Acid Biosynthesis
P value
3e-07
2e-01
5e-01
Enrichment Ratio
L
Relative mRNA expression
ACC
SREBP1c
FASN
PPARγ
LXRα
DGAT1
DGAT2
PPARα
CPT1
MCD
LACD
CD36
M
Littermate
Rarres2-/-
PPARγ
SCD1
HSP90
53KDa
40KDa
90KDa
Relative protein level (fold Littermate)

Figure 5. Chemerin knockout causes metabolic substrate inflexibility and cardiac metabolic dysfunction in HFD mice

Rarres2$^{-/-}$ and Littermate WT mice were subjected to high-fat diet feeding for 20 weeks. Calorimetric parameters about male *Rarres2*$^{-/-}$ and WT littermate mice were individually placed in the metabolic cages for 2-3 days of measurement; (A) oxygen consumption; (B) carbon dioxide production; (C) Respiratory exchange ratio (RER).

(D) Daily locomotor activity, n = 5. *p < 0.05, (E-I) Serum levels of NEFA, TG, TC, HDL-C, and No HDL-C in *Rarres2*$^{-/-}$ and littermate mice, n = 6.

(J) Metabolic Heatmap and hierarchical clustering of lipid metabolites in the heart of *Rarres2*$^{-/-}$ and littermate mice.

(K)Top metabolic pathways enriched in *Rarres2*$^{-/-}$ mice identified by Molecular Pathway Level Analysis (false discovery rate<0.05).

(L) mRNA expression levels of lipogenic genes, n = 6.

(M) Representative Western blots and their quantification of PPARγ and SCD1. The HSP90 was used as a loading control (n = 7). *p < 0.05, **p < 0.01.

Emerging evidence aimed at disclosing the microenvironment of adipose tissues and its potential impact on systemic metabolism has shed light on the pathogenesis of obesity-linked cardiovascular diseases. Adipose tissue function as an endocrine organ by secreting multiple immune-modulatory proteins known as adipokines.[25] Recent clinical studies demonstrated that a higher recurrence rate of obesity-related cardiomyopathy was associated with adipose tissue dysfunction,[26] such as an increment in serum chemerin.[27] Chemerin is a novel adipokine that is highly linked to inflammation and adipogenesis.[28] In addition to this, chemerin is also well-known as a biomarker in cardiovascular diseases (CVDs), especially in obese and diabetic hearts.[29] Given that there exist potential links among obesity, adipokines, and the heart, we investigated the role of chemerin in obese-related cardiomyopathy.

Firstly, in HFD mice, serum chemerin was mainly secreted in adipose tissues compared with other tissues (e.g., liver, skeletal muscle, and heart) (Figure S2). This is consistent with previous studies.[30,31] And, we then hypothesized that an increasement of serum adipokine chemerin could stimulate the expression of its main receptor CMKLR1, and this early event might be an endogenous protective factor against obesity-related cardiomyopathy. Accordingly, chemerin (*Rarres2*) knockout mice under high-fat feeding led to the development of lipotoxicity, and contributed to an impairment of insulin sensitivity and an evoked inflammation, eventually resulting in cardiac dysfunction (Figure 3). Of note, these abnormalities above were not found in *Rarres2* knockout mice under normal-diet feeding. Next, in lipid-overloaded cardiomyocytes, chemerin supplementation prevented lipid accumulation and inflammation, and knocking down the *CMKLR1* gene completely abolished these effects (Figure 6). Therefore, our present data obtained strongly demonstrate that adipocyte-derived chemerin lowered lipotoxicity and inflammation, and restored cardiac dysfunction in the obese/or pre-diabetic heart. Chemerin, an endogenous cardioprotective factor in the presence of obesity, was suggested to protect against high-fat diet-induced cardiac dysfunction. *In vitro* study, we further found that adding exogenous chemerin into a high palmitate-cultured medium could protect cardiac myocytes from lipotoxicity and insulin resistance, indicating that chemerin might be a potential clinical translation target against obesity-related cardiomyopathy. Here, we will briefly discuss these findings above.

The current work showed that *Rarres2*$^{-/-}$ mice fed with HFD contributed to higher body weight (Figure 3A), and impaired insulin sensitivity (e.g., GTT and ITT) (Figures 3B and 3C). Also, these abnormalities were accompanied by impairments of insulin signaling and glucose-dependent insulin secretion.[32] Contrary to these findings, several recent studies showed adipokine chemerin could induce insulin resistance in rat cardiomyocytes, and it suggested that chemerin potentially plays a dual role in different stimuli and experimental conditions as to its effects on the heart.[33–35] In the present study, we also indicated that lipid overloaded cardiomyocytes supplemented with 200 ng/mL chemerin prevented lipid-induced insulin resistance (e.g., insulin-stimulated Akt phosphorylation at Ser473), and lowered phosphorylation of both kinases P38 MAP kinase and ERK1/2. On the contrary, Henrike Sell et al. showed that chemerin could decrease insulin sensitivity in skeletal muscle cells through ERK activation, and this was accompanied by activated NF-κB pathway and MAP kinases.[36] Although the present study suggests adipocyte-derived chemerin functions as a potential protective regulator of cardiac function in HFD mice, these different results remain that adipokine chemerin might be a double-edged sword in the obese/or pre-diabetic heart.[15]

Considering the potential roles of chemerin in lipid metabolism, we speculate that adipokine chemerin influences the expression of peroxisome proliferator-activated receptor (PPARγ) directly or indirectly. PPARγ is a well-known transcription factor in lipid metabolism, it leads to an increment of lipid uptake through mediating lipid transporter (e.g., CD36) and storages as lipid droplets in the heart.[16] Shanmugamet et al. showed there was a strong association between PPARγ and chemerin during adipogenesis of bone marrow-derived mesenchymal stem cells, and further revealed the chemerin promoter was positively

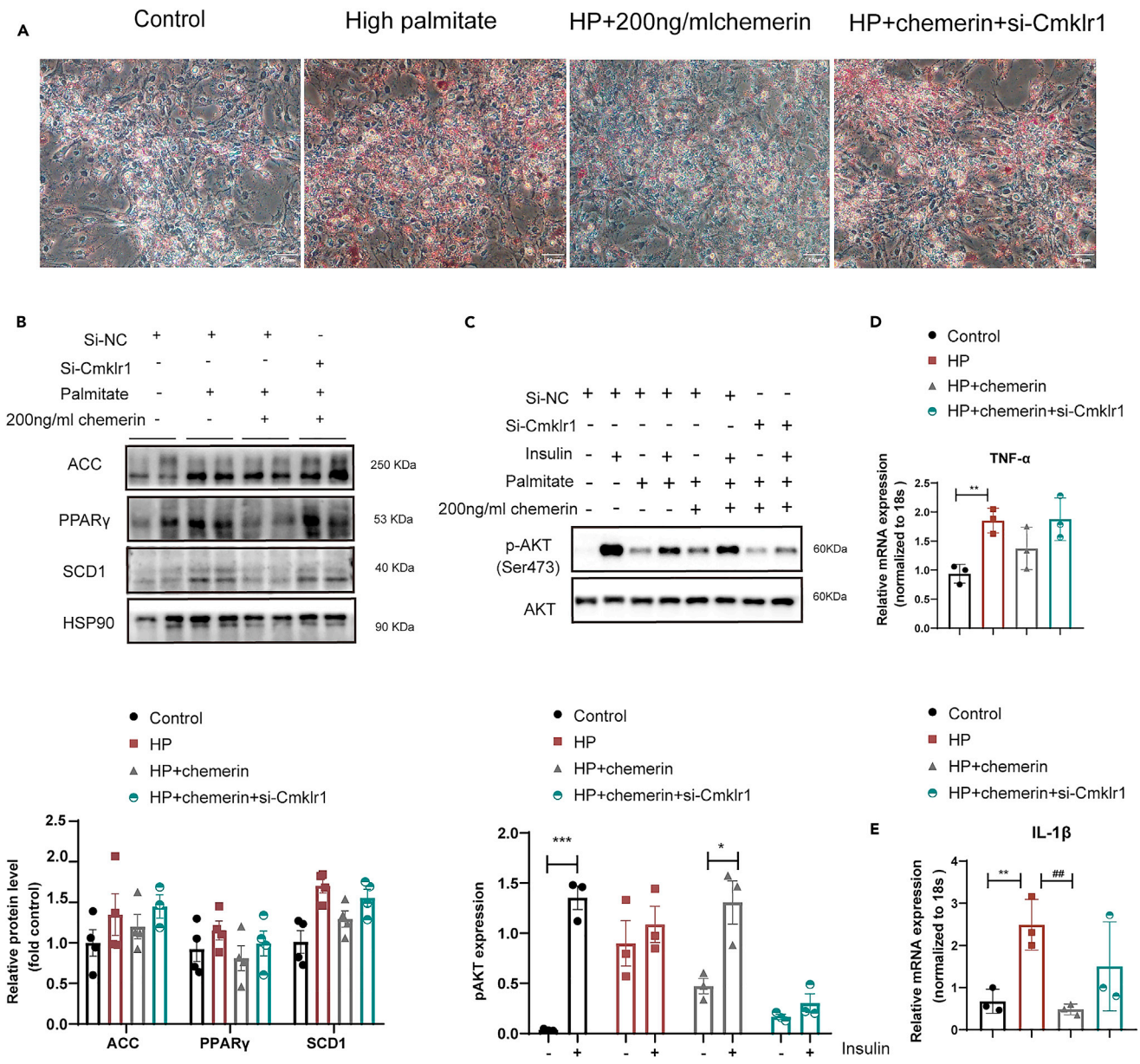

Figure 6. Chemerin supplementation restores lipid overload-induced lipotoxicity and inflammation in cardiomyocytes

Neonatal mouse primary cardiomyocytes (NMCMs) were first exposed to a control medium, high palmitate medium (HP) for 12h, and then treated with either 200 ng/ml chemerin or si-*CMKLR1* for another 24h.

(A) Cells were stained with Oil red O.Scale bar = 50μm.

(B) Representative Western blots and its quantification of lipids metabolism enzymes (e.g., ACC, SCD1, and PPARγ), n = 4.

(C) Representative Western blots and its quantification of phosphorylation AKT (*p*-AKT ser 473). The HSP90 was used as a loading control (n = 3).

(D and E) mRNA expressions of pro-inflammatory cytokines (e.g., *TNFα* and *IL-1β*), n = 3.

regulated by a PPARγ sequence.[37] Indeed, chemerin could reduce cardiac PPARγ levels, concomitantly attenuating cardiac lipotoxicity, which is one of the mechanisms responsible for obese-related cardiomyopathy and heart failure.[38] In this study, *Rarres2*$^{-/-}$ mice fed with HFD significantly increased mRNA expressions of both *PPARγ* and PPAR-dependent genes (e.g., *CD36*, *Fabp4*, and *Fasn*). These altered PPAR-dependent genes might be interpreted as a compensatory mechanism in response to increased lipid accumulation.[31] However, concerning the potential link between adipokine chemerin and PPARγ in the heart, it still needs to be further clarified in the future.

Limitations of the study

The present study has several limitations, as follows: First, a global *Rarres2* knockout model was employed in this study, and we could not accurately observe the effect of specific tissue-secreted chemerin deficiency on cardiac function. Nevertheless, chemerin is a secretory protein mainly produced by adipose tissue, and chemerin receptor CMKLR1 conditional knockout in the heart should be considered in future studies. Second, we did not investigate potential mechanisms of chemerin in obese-related cardiomyopathy. Accordingly, we observed a significant regulator of cardiomyocyte lipid metabolism, such as PPARγ, was significantly increased in *Rarres2*$^{-/-}$mice under high-fat feeding. Given that PPARγ is a transcription factor that regulates fatty acid transport and lipid droplet formation,[39] future work will be considered to investigate the upstream regulator of PPARγ that is involved in chemerin signaling.

STAR★METHODS

Detailed methods are provided in the online version of this paper and include the following:

- KEY RESOURCES TABLE
- RESOURCE AVAILABILITY
  - Lead contact
  - Materials availability
  - Data and code availability
- METHOD DETAILS
  - Experimental model and subject details
  - Echocardiography
  - Histopathology
  - Oil-Red O staining
  - Western blotting
  - Real-time qPCR (RT-qPCR)
  - Isolation and culturing of neonatal mice ventricular myocytes (NMVMs)
  - Transfection with siRNA
  - Glucose insulin tolerance tests
  - Serum ELISA and biochemistry detection
  - Energy expenditure and locomotor activity
  - Gas chromatography-mass spectrometry (GC-MS) analysis
  - Quantification and statistical analysis

SUPPLEMENTAL INFORMATION

Supplemental information can be found online at https://doi.org/10.1016/j.isci.2023.106495.

ACKNOWLEDGMENTS

Many thanks to my colleagues in the department of Cardiology, Children's Hospital of Chongqing Medical University, and the Obesity-Related Diseases Research Unit of Chongqing Medical University.

This study was sponsored by the National Key R&D Program of China (No. 2018YFA0800401 to Xi Li); National Natural Science Foundation of China (No. 81770861, 82070899 and 82011530460 to Xi Li, 81974030 to Jie Tian, 8210033375 to Shujin Wang); Natural sciences foundation of Chongqing (No. CSTB2022NSCQ-MSX0827 to Jie Tian, 2022NSCQ-MSX0643 to Shujin Wang); Key Grant from the National Clinical Research Center for Child Health and Disorders (Grant No. NCRCCHD-2021-KP-01 to Jie Tian). Scientific and Technological Research Program of Chongqing Municipal Education Commission (Grant No. KJQN202200445, KJQN202100410 to Shujin Wang); CQMU Program for Youth Innovation in Future Medicine (W0046) .

AUTHOR CONTRIBUTIONS

Conceptualization: R.M.L and S.J.W; methodology: R.M.L, Y.Y.H, and M.Q.H; resources: CLH and RC; writing – original draft, R.M.L.; writing –review & editing, S.J.W., X.L., and J.T; project administration: S.J.W. and X.L.; funding acquisition: J.T., X,L., and S.J.W.

DECLARATION OF INTERESTS

The authors declare no conflict of interest.

Received: December 8, 2022
Revised: February 23, 2023
Accepted: March 22, 2023
Published: March 24, 2023

REFERENCES

1. Isfort, M., Stevens, S.C.W., Schaffer, S., Jong, C.J., and Wold, L.E. (2014). Metabolic dysfunction in diabetic cardiomyopathy. Heart Fail. Rev. *19*, 35–48. https://doi.org/10.1007/s10741-013-9377-8.

2. Liu, Y., Steinbusch, L.K.M., Nabben, M., Kapsokalyvas, D., van Zandvoort, M., Schönleitner, P., Antoons, G., Simons, P.J., Coumans, W.A., Geomini, A., et al. (2017). Palmitate-induced vacuolar-type H(+)-ATPase inhibition feeds forward into insulin resistance and contractile dysfunction. Diabetes *66*, 1521–1534. https://doi.org/10.2337/db16-0727.

3. Alpert, M.A. (2001). Obesity cardiomyopathy: pathophysiology and evolution of the clinical syndrome. Am. J. Med. Sci. *321*, 225–236. https://doi.org/10.1097/00000441-200104000-00003.

4. Wang, S., Wong, L.Y., Neumann, D., Liu, Y., Sun, A., Antoons, G., Strzelecka, A., Glatz, J.F.C., Nabben, M., and Luiken, J.J.F.P. (2020). Augmenting vacuolar H(+)-ATPase function prevents cardiomyocytes from lipid-overload induced dysfunction. Int. J. Mol. Sci. *21*, 1520.

5. Seferović, P.M., and Paulus, W.J. (2015). Clinical diabetic cardiomyopathy: a two-faced disease with restrictive and dilated phenotypes. Eur. Heart J. *36*, 1718-1727–1727a-1727c. https://doi.org/10.1093/eurheartj/ehv134.

6. Scheja, L., and Heeren, J. (2019). The endocrine function of adipose tissues in health and cardiometabolic disease. Nat. Rev. Endocrinol. *15*, 507–524. https://doi.org/10.1038/s41574-019-0230-6.

7. Oikonomou, E.K., and Antoniades, C. (2019). The role of adipose tissue in cardiovascular health and disease. Nat. Rev. Cardiol. *16*, 83–99. https://doi.org/10.1038/s41569-018-0097-6.

8. Longo, M., Zatterale, F., Naderi, J., Parrillo, L., Formisano, P., Raciti, G.A., Beguinot, F., and Miele, C. (2019). Adipose tissue dysfunction as determinant of obesity-associated metabolic complications. Int. J. Mol. Sci. *20*, 2358. https://doi.org/10.3390/ijms20092358.

9. Ren, Y., Zhao, H., Yin, C., Lan, X., Wu, L., Du, X., Griffiths, H.R., and Gao, D. (2022). Adipokines, hepatokines and myokines: focus on their role and molecular mechanisms in adipose tissue inflammation. Front. Endocrinol. *13*, 873699. https://doi.org/10.3389/fendo.2022.873699.

10. Ray, I., Mahata, S.K., and De, R.K. (2016). Obesity: an immunometabolic perspective. Front. Endocrinol. *7*, 157. https://doi.org/10.3389/fendo.2016.00157.

11. Packer, M. (2018). Epicardial adipose tissue may mediate deleterious effects of obesity and inflammation on the myocardium. J. Am. Coll. Cardiol. *71*, 2360–2372. https://doi.org/10.1016/j.jacc.2018.03.509.

12. Chang, S.S., Eisenberg, D., Zhao, L., Adams, C., Leib, R., Morser, J., and Leung, L. (2016). Chemerin activation in human obesity. Obesity *24*, 1522–1529. https://doi.org/10.1002/oby.21534.

13. Hsu, L.A., Chou, H.H., Teng, M.S., Wu, S., and Ko, Y.L. (2021). Circulating chemerin levels are determined through circulating platelet counts in nondiabetic Taiwanese people: a bidirectional Mendelian randomization study. Atherosclerosis *320*, 61–69. https://doi.org/10.1016/j.atherosclerosis.2021.01.014.

14. Goralski, K.B., McCarthy, T.C., Hanniman, E.A., Zabel, B.A., Butcher, E.C., Parlee, S.D., Muruganandan, S., and Sinal, C.J. (2007). Chemerin, a novel adipokine that regulates adipogenesis and adipocyte metabolism. J. Biol. Chem. *282*, 28175–28188. https://doi.org/10.1074/jbc.M700793200.

15. Bondue, B., Wittamer, V., and Parmentier, M. (2011). Chemerin and its receptors in leukocyte trafficking, inflammation and metabolism. Cytokine Growth Factor Rev. *22*, 331–338. https://doi.org/10.1016/j.cytogfr.2011.11.004.

16. Goto, K., Iso, T., Hanaoka, H., Yamaguchi, A., Suga, T., Hattori, A., Irie, Y., Shinagawa, Y., Matsui, H., Syamsunarno, M.R.A.A., et al. (2013). Peroxisome proliferator-activated receptor-gamma in capillary endothelia promotes fatty acid uptake by heart during long-term fasting. J. Am. Heart Assoc. *2*, e004861. https://doi.org/10.1161/JAHA.112.004861.

17. Leiherer, A., Muendlein, A., Kinz, E., Vonbank, A., Rein, P., Fraunberger, P., Malin, C., Saely, C.H., and Drexel, H. (2016). High plasma chemerin is associated with renal dysfunction and predictive for cardiovascular events - insights from phenotype and genotype characterization. Vascul. Pharmacol. *77*, 60–68. https://doi.org/10.1016/j.vph.2015.08.010.

18. Eichelmann, F., Schulze, M.B., Wittenbecher, C., Menzel, J., Weikert, C., di Giuseppe, R., Biemann, R., Isermann, B., Fritsche, A., Boeing, H., and Aleksandrova, K. (2019). Chemerin as a biomarker linking inflammation and cardiovascular diseases. J. Am. Coll. Cardiol. *73*, 378–379. https://doi.org/10.1016/j.jacc.2018.10.058.

19. Herová, M., Schmid, M., Gemperle, C., Loretz, C., and Hersberger, M. (2014). Low dose aspirin is associated with plasma chemerin levels and may reduce adipose tissue inflammation. Atherosclerosis *235*, 256–262. https://doi.org/10.1016/j.atherosclerosis.2014.05.912.

20. İnci, S., Aksan, G., and Doğan, P. (2016). Chemerin as an independent predictor of cardiovascular event risk. Ther. Adv. Endocrinol. Metab. *7*, 57–68. https://doi.org/10.1177/2042018816629894.

21. Zhou, X., Tao, Y., Chen, Y., Xu, W., Qian, Z., and Lu, X. (2019). Serum chemerin as a novel prognostic indicator in chronic heart failure. J. Am. Heart Assoc. *8*, e012091. https://doi.org/10.1161/JAHA.119.012091.

22. Brankovic, M., Akkerhuis, K.M., Mouthaan, H., Brugts, J.J., Manintveld, O.C., van Ramshorst, J., Germans, T., Umans, V., Boersma, E., and Kardys, I. (2018). Cardiometabolic biomarkers and their temporal patterns predict poor outcome in chronic heart failure (Bio-SHiFT study). J. Clin. Endocrinol. Metab. *103*, 3954–3964. https://doi.org/10.1210/jc.2018-01241.

23. Zhang, O., Ji, Q., Lin, Y., Wang, Z., Huang, Y., Lu, W., Liu, X., Zhang, J., Liu, Y., and Zhou, Y.J. (2015). Circulating chemerin levels elevated in dilated cardiomyopathy patients with overt heart failure. Clin. Chim. Acta *448*, 27–32. https://doi.org/10.1016/j.cca.2015.05.018.

24. Virani, S.S., Alonso, A., Benjamin, E.J., Bittencourt, M.S., Callaway, C.W., Carson, A.P., Chamberlain, A.M., Chang, A.R., Cheng, S., Delling, F.N., et al. (2020). Heart disease and stroke statistics-2020 update: a report from the American Heart Association. Circulation *141*, e139–e596. https://doi.org/10.1161/CIR.0000000000000757.

25. Nakamura, K., Fuster, J.J., and Walsh, K. (2014). Adipokines: a link between obesity and cardiovascular disease. J. Cardiol. *63*, 250–259. https://doi.org/10.1016/j.jjcc.2013.11.006.

26. Schrover, I.M., van der Graaf, Y., Spiering, W., and Visseren, F.L.; SMART study group (2018). The relation between body fat distribution, plasma concentrations of adipokines and the metabolic syndrome in patients with clinically manifest vascular disease. Eur. J. Prev. Cardiol. *25*, 1548–1557. https://doi.org/10.1177/2047487318790722.

27. Piché, M.E., Tchernof, A., and Després, J.P. (2020). Obesity phenotypes, diabetes, and cardiovascular diseases. Circ. Res. *126*, 1477–1500. https://doi.org/10.1161/CIRCRESAHA.120.316101.

28. Kukla, M., Mazur, W., Bułdak, R.J., and Zwirska-Korczala, K. (2011). Potential role of leptin, adiponectin and three novel adipokines–visfatin, chemerin and vaspin–in chronic hepatitis. Mol. Med. *17*, 1397–1410. https://doi.org/10.2119/molmed.2010.00105.

29. Ferland, D.J., and Watts, S.W. (2015). Chemerin: a comprehensive review elucidating the need for cardiovascular research. Pharmacol. Res. *99*, 351–361. https://doi.org/10.1016/j.phrs.2015.07.018.

30. Léniz, A., González, M., Besné, I., Carr-Ugarte, H., Gómez-García, I., and Portillo, M.P. (2022). Role of chemerin in the control of glucose homeostasis. Mol. Cell. Endocrinol. *541*, 111504. https://doi.org/10.1016/j.mce.2021.111504.

31. Rourke, J.L., Dranse, H.J., and Sinal, C.J. (2013). Towards an integrative approach to understanding the role of chemerin in human health and disease. Obes. Rev. *14*, 245–262. https://doi.org/10.1111/obr.12009.

32. Takahashi, M., Okimura, Y., Iguchi, G., Nishizawa, H., Yamamoto, M., Suda, K., Kitazawa, R., Fujimoto, W., Takahashi, K., Zolotaryov, F.N., et al. (2011). Chemerin regulates beta-cell function in mice. Sci. Rep. *1*, 123. https://doi.org/10.1038/srep00123.

33. Zhang, R., Liu, S., Guo, B., Chang, L., and Li, Y. (2014). Chemerin induces insulin resistance in rat cardiomyocytes in part through the ERK1/2 signaling pathway. Pharmacology *94*, 259–264. https://doi.org/10.1159/000369171.

34. Rodríguez-Penas, D., Feijóo-Bandín, S., García-Rúa, V., Mosquera-Leal, A., Durán, D., Varela, A., Portolés, M., Roselló-Lletí, E., Rivera, M., Diéguez, C., et al. (2015). The adipokine chemerin induces apoptosis in cardiomyocytes. Cell. Physiol. Biochem. *37*, 176–192. https://doi.org/10.1159/000430343.

35. Ferland, D.J., Seitz, B., Darios, E.S., Thompson, J.M., Yeh, S.T., Mullick, A.E., and Watts, S.W. (2018). Whole-body but not hepatic knockdown of chemerin by antisense oligonucleotide decreases blood pressure in rats. J. Pharmacol. Exp. Ther. *365*, 212–218. https://doi.org/10.1124/jpet.117.245456.

36. Sell, H., Laurencikiene, J., Taube, A., Eckardt, K., Cramer, A., Horrighs, A., Arner, P., and Eckel, J. (2009). Chemerin is a novel adipocyte-derived factor inducing insulin resistance in primary human skeletal muscle cells. Diabetes *58*, 2731–2740. https://doi.org/10.2337/db09-0277.

37. Muruganandan, S., Parlee, S.D., Rourke, J.L., Ernst, M.C., Goralski, K.B., and Sinal, C.J. (2011). Chemerin, a novel peroxisome proliferator-activated receptor gamma (PPARgamma) target gene that promotes mesenchymal stem cell adipogenesis. J. Biol. Chem. *286*, 23982–23995. https://doi.org/10.1074/jbc.M111.220491.

38. Abel, E.D., Litwin, S.E., and Sweeney, G. (2008). Cardiac remodeling in obesity. Physiol. Rev. *88*, 389–419. https://doi.org/10.1152/physrev.00017.2007.

39. Montaigne, D., Butruille, L., and Staels, B. (2021). PPAR control of metabolism and cardiovascular functions. Nat. Rev. Cardiol. *18*, 809–823. https://doi.org/10.1038/s41569-021-00569-6.

40. Lin, Y., Yang, X., Liu, W., Li, B., Yin, W., Shi, Y., and He, R. (2017). Chemerin has a protective role in hepatocellular carcinoma by inhibiting the expression of IL-6 and GM-CSF and MDSC accumulation. Oncogene *36*, 3599–3608. https://doi.org/10.1038/onc.2016.516.

41. Wang, S., Fu, W., Zhao, X., Chang, X., Liu, H., Zhou, L., Li, J., Cheng, R., Wu, X., Li, X., and Sun, C. (2022). Zearalenone disturbs the reproductive-immune axis in pigs: the role of gut microbial metabolites. Microbiome *10*, 234. https://doi.org/10.1186/s40168-022-01397-7.

42. Wang, S., Schianchi, F., Neumann, D., Wong, L.Y., Sun, A., van Nieuwenhoven, F.A., Zeegers, M.P., Strzelecka, A., Col, U., Glatz, J.F.C., et al. (2021). Specific amino acid supplementation rescues the heart from lipid overload-induced insulin resistance and contractile dysfunction by targeting the endosomal mTOR-v-ATPase axis. Mol. Metab. *53*, 101293. https://doi.org/10.1016/j.molmet.2021.101293.

43. Sreejit, P., Kumar, S., and Verma, R.S. (2008). An improved protocol for primary culture of cardiomyocyte from neonatal mice. In Vitro Cell. Dev. Biol. Anim. *44*, 45–50. https://doi.org/10.1007/s11626-007-9079-4.

44. Sun, Y., Hao, L., Han, W., Luo, J., Zheng, J., Yuan, D., Ye, H., Li, Q., Huang, G., Han, T., and Yang, Z. (2023). Intrafollicular fluid metabolic abnormalities in relation to ovarian hyperstimulation syndrome: follicular fluid metabolomics via gas chromatography-mass spectrometry. Clin. Chim. Acta *538*, 189–202. https://doi.org/10.1016/j.cca.2022.11.033.

STAR★METHODS

KEY RESOURCES TABLE

REAGENT or RESOURCE	SOURCE	IDENTIFIER
Antibodies		
Chemerin	Santa Cruz	tsc-373797;RRID:AB_10947246
CMKLR1	Abcepta	AP50620;RRID:AB_2550816
HSP90	Cell Signaling	4877s;RRID: AB_2233307
PPARγ	Cell Signaling	2443SRRID:AB_823598
p-P38	Cell Signaling	4511S;RRID:AB_2139682
P38	Cell Signaling	9212S;RRID: AB_330713
p-P65	Cell Signaling	3033SRRID: AB_331284
P65	Cell Signaling	8242SRRID: AB_10859369
p-Akt	Cell Signaling	4058S;RRID:AB_331168
Akt	Cell Signaling	9272SRRID:AB_329827
Chemicals,Peptides,and Recombinant Proteins		
Wheat germ agglutinin (WGA)	Sigma	L4895
Oil Red O	Sigma	O0625
BCA Protein Assay Kit	Beyotime	P0009
Chemerin ELISA kit	R&D Systems	Cat.DY2325
Triglyceride assay kit	Jiancheng Bioengineering	A110-1-1
Nonesterified Free FAtty acids assay kit	Jiancheng Bioengineering	A042-2-1
High-density lipoprotein cholesterol assay kit	Jiancheng Bioengineering	A112-1-1
collagenase II	Worthington	LS004176
Short interfering RNAs (siRNA) for CMKLR1	Gene Pharma	K01
Recombinant Human Chemerin	PeproTech	300-66
lipofectamine-RNAIMAX	Invitrogen	13778150
Experimental models: Organism/Strains		
Rarres2 knock out mice	Dr. Rui He	Department of immunology, Fudan University.
neonatal mice ventricular myocytes	Tian Lab	This paper
Other		
TSE Systems	Lab Master	PhenoMaster _H
Vevo 3100 LT	FUJIFILM	3100

RESOURCE AVAILABILITY

Lead contact

Further information on resources and reagents should be directed to the lead contact, professor jietian (jietian@cqmu.edu.cn).

Materials availability

This study did not generate new unique reagents.

Data and code availability

Not applicable.

METHOD DETAILS

Experimental model and subject details

Eight-week-old C57BL/6J male mice were purchased from the Experimental Animal Center of Chongqing Medical University. *Rarres2*$^{-/-}$ mice were kindly provided by Dr. Rui He (Department of Immunology, Biotherapy Research Center, Fudan University).[40] All animal experiment procedures were approved by the Animal Care and Use Committee of Chongqing Medical University. Wild Type mice (n=6) were fed with normal diet or high fat diet for 20 weeks. *Rarres2*$^{-/-}$ mice homozygous and their wild-type (WT) littermates were identified by PCR. Eight-week-old male *Rarres2*$^{-/-}$ mice and WT littermates were studied. Mice were fed with a normal diet (n=6) (Rodent Growth and Breeding Feed, Beijing KEAO XIELI FEED CO., LTD) or high-fat diet (n=8) (HFD, 60%kal fat from Research Diet Inc, D12492) for 20 weeks in a 12-hour cycle environment.

Echocardiography

Mice were placed gently on the anesthesia machine and anesthetized with inhaled isoflurane. Heart rate in mice maintained at 450-500bpm. Two-dimensional (2D) guided M-mode echocardiography was performed using an echocardiogram (Vevo 3100 Imaging System, VisualSonics, Toronto, Canada) equipped with a 30-MHz linear transducer. B-Mode Image of the Parasternal Short Axis View can get Left ventricular posterior wall end diastole and end systole (LVPWd, LVPWs), Left ventricular internal diameter end diastole and end systole (LVIDd, LVIDs). PW Doppler Mode waveform of mitral valve flow in the apical four-chamber view to get Mitral isovolumic relaxation and contraction times (IVRT, IVCT), Peak early, and atrial filling (Peak E, Peak A).

Histopathology

The middle segment of the fresh heart was put in 4% paraformaldehyde for 24h and then cut several crosses sections from paraffin-embedded specimens. Next, H&E and Masson trichrome staining were used to observe cardiac morphology and collagen deposition. Each staining was performed on the slides of three mice in each group. Wheat germ agglutinin (WGA) staining (Sigma L4895, dilute 1:500) was performed to observe Myocardial Hypertrophy. Microscopy detection and collection images by Fluorescent Microscopy, excitation wavelength 465-495 nm and emission wavelength 515-555 nm. Image J software (ImageJ1.8.0.345, National Institutes of Health, Bethesda, MD, USA) was used for the area of cardiomyocyte analysis.

Oil-Red O staining

The Oil-Red O staining was used for the determination of lipid deposition *In vitro* and *in vivo*. NMVMs cells were fixed in 4% paraformaldehyde for 20 min and stained with Oil-Red O for 120 min. The 10 μm serial cryosections of heart cross segments were prepared in a cryostat (Leica CM3050 S, Leica, Wetzlar, Germany) at −20°C, fixed in 4% paraformaldehyde, rinsed with 60% isopropanol and stained with 0.3% Oil-Red O (Sigma Aldrich, USA) for 20 min at room temperature.

Western blotting

Heart tissues were prepared according to a previously published method.[41] Briefly, heart tissues were homogenized in cell lysis buffer and quantified for protein levels using a commercial assay Enhanced BCA Protein Assay Kit (Beyotime, Jiangsu, China). Protein samples (20 μg) were electrophoresed by sodium dodecyl sulfate (SDS) polyacrylamide gel (10~12%) and transferred to a nitrocellulose membrane (Millipore). Membranes were blocked with 5% experimental grade skimmed milk in Tris-buffer saline (TBS), Primary antibodies (Table S1) were used in TBST with 3% BSA overnight at 4°C, and secondary antibody was added at 1:10000 for 1 h at room temperature (Jackson Immunoassay, USAPA). Amersham Imager 600 Analysis Software was used to quantify signals.

Real-time qPCR (RT-qPCR)

Total RNA was extracted from hearts using Trizol reagent (Thermo Fisher Scientific, Carlsbad, CA, USA) in accordance with previous description.[42] cDNA was synthesized from total RNA using the RevertAid First Strand cDNA Synthesis Kit (Thermo Fisher Scientific, Vilnius, Lithuania) as per the manufacturer's instructions. The total RNA quantity was determined by SYBR Green Master Mix (Thermo Fisher Scientific, Vilnius, Lithuania). The primer sequences used are shown in Table S2.

Isolation and culturing of neonatal mice ventricular myocytes (NMVMs)

Primary neonatal cardiomyocytes from mice were performed as previously described.[43] Briefly, primary myocytes were adopted from neonatal mice within three days. Hearts were excised and immediately transferred into ice-cold phosphate-buffered saline (PBS; Ca^{2+} and Mg^{2+} free). After blood was squeezed out, the hearts were cut into pieces and digested by 0.05% collagenase II (Worthington, LS004176) gently. Finally, cardiomyocytes were collected by centrifuging in a specific density gradient. The myocyte-enriched suspension was plated onto culture dishes at a density of 5×10^5 cells per cm^2 and treated in F12/DMEM (1:1) containing 10% FBS,1% penicillin, and streptomycin,0.1g/L 5-Fluorouracil. The cells were incubated in a 5% CO_2 incubator at 37°C. After adhesion 48h, cells were treated with control medium, low-palmitate medium (LP; 20 μM palmitate; palmitate/BSA ratio 0.3:1), high-palmitate medium (HP; 200 μM palmitate; palmitate/BSA ratio 3:1) or HP medium with 200ng/ml chemerin (PeproTech,300-66) for 24h.[4]

Transfection with siRNA

The short interfering RNAs (siRNA) for *CMKLR1* (5′-CCGGCAUCUAUGAUGAUGATT-3′) were chemically synthesized by Gene Pharma (Shanghai, China). NMVMs were transfected with Negative Control (NC) siRNA and targeted CMKLR1 using lipofectamine-RNAIMAX (Invitrogen, Carlsbad, CA, USA) according to the Invitrogen protocol. Cells were kept for 48h, and transfection was evaluated by Western blot.

Glucose insulin tolerance tests

Both glucose tolerance test (GTT) and insulin tolerance test (ITT) were performed on the mice preceding treatment with normal or HFD for 18 weeks. For GTT, mice fasted overnight for 12-16 h and then were administered 2 g/kg body weight D-glucose (intraperitoneal Injection). Afterward, blood glucose from the tail was measured by a glucometer (OneTouch UltraEasy, LifeScan, Inc). For ITT, food was removed from mice 4 h before the experiment, and recombinant insulin (Novo Nordisk A/S, Bagsvaerd, Denmark) was administered (intraperitoneal Injection) at 0.75U/kg. Area-under-curve (AUC) was calculated by the trapezoid rule.

Serum ELISA and biochemistry detection

Animals were fasted overnight before being anesthetized in isoflurane-saturated chambers, and blood samples were collected from mouse eyes following anesthesia. After 20 minutes at room temperature, the blood was centrifuged at 3,000 g at 4°C. Supernatants were collected after centrifugation for further analysis. The mice serum chemerin was assessed by ELISA kit from R&D System (Cat.DY2325; R&D Systems, Minneapolis, MN, USA) and was performed according to the instruction. The serum levels of TG, TC, FFA and HDL-C were determined by the detection kit purchased from Nanjing Jiancheng Bioengineering Institute (Nanjing, China).

Energy expenditure and locomotor activity

For calorimetric analyses, mice were acclimated to metabolic cages one week after being fed with 16 weeks of HFD. Energy expenditure was measured using a computer-controlled indirect calorimetry system (LabMaster; TSE Systems) run by the EBGM Core. O_2 consumption and CO_2 production were measured for 1 min at 27 min intervals for each animal. The respiratory exchange ratio (RER) was calculated as the ratio of CO_2 production to O_2 consumption. Light and dark cycle energy expenditure were determined using the average of all 72 data points per 12 h light cycle of 3 consecutive days. In turn, these were averaged to obtain a total 24 h energy expenditure. Locomotor activity was determined with infrared sensor pairs arranged in a grid pattern for horizontal (x, y level) activity. The movement was monitored continuously, reported as a total count every 9 min, and expressed as counts per 24h.

Gas chromatography-mass spectrometry (GC-MS) analysis

Gas chromatography-mass spectrometry (GC-MS) Analysis was performed by the Key Laboratory of Maternal and Fetal Medicine of Chongqing Municipality (The First Affiliated Hospital of Chongqing Medical University, Chongqing, China), as described previously.[44] Briefly, GC–MS Analysis Samples were run on an Agilent 7890B gas chromatography system with an Agilent 5977A MSD system (Agilent Technologies Inc., CA, USA). The separation was carried out on a 30 m × 0.25 mm DB-5MS (film thickness 0.25 μm, Agilent J & W Scientific, Folsom, CA, USA) fused-silica capillary column. The carrier gas was helium (99.999%), and the flow rate was 1.5 mL/min. The injector temperature was 260°C, injection volume was 1 μL, and sample injection was made in splitless mode. The solvent delay time was set at 5 min. The column temperature

started at 60°C, ramped to 125°C at a rate of 8°C /min, to 210°C at a rate of 5°C /min, to 270°C at a rate of 10°C /min, to 305°C at a rate of 20°C /min, and finally held at 305°C for 5 min. The temperature of the MS quadrupole and ion source (electron impact) was set to 150°C and 230°C, respectively, and the collision energy was 70 eV. The mass spectrometry data were obtained in the full-scan mode with the m/z range of 50-500. The QCs were injected every 15 samples throughout the run to provide a set of data from which repeatability could be assessed.

Quantification and statistical analysis

Comparisons of continuous variables were performed using an unpaired two-sample t-test, as appropriate. *P*-values <0.05 were considered statistically significant. To compare more than two groups, one-way analysis of variance (ANOVA) with Duncan's multiple comparison option was used in this study. All analyses were performed with GraphPad Prism Software (version 8.03, Inc, San Diego, CA, USA). In addition, for the data of qPCR and GC-MS, outliers were firstly excluded using Grubb's outlier test with α=0.05. To ensure normal distribution, the data of qPCR were $\log_2$-transformed and Pst titer data of GC-MS (Untargeted Metabolomics) were $\log_{10}$-transformed. The normal distribution of all data sets was verified using the Shapiro-Wilk test with α=0.01. Subsequently, the data were analyzed using one-way ANOVA analyses with Tukey's multiple testing correction. Differences were considered significant with α=0.05.